Journal of
Mechanical
Science and
Technology

Journal of Mechanical Science and Technology 21 (2007) 1352~1358

Numerical Simulation of Fish Motion by Using Lattice Boltzmann-Immersed Boundary Velocity Correction Method

Chang Shu[a,*], Ningyu Liu[a], Yongtian Chew[a], Zhiliang Lu[b]

[a]*Department of Mechanical Engineering, National University of Singapore, 119260, Singapore*

[b]*Department of Aerodynamics, Nanjing University of Aeronautic and Astronautics, Nanjing, China*

(Manuscript Received October 4, 2006; Revised April 2, 2007; Accepted May 2, 2007)

Abstract

Numerical simulation of a flow past an undulating two-dimensional fish-like body is carried out by using Lattice Boltzmann Method (LBM) and our newly-proposed Immersed Boundary Velocity Correction Method (IBVCM). The fish body used in the simulation is constructed from the NACA0012 airfoil. Based on the kinematics for undulatory swimming fish, the midline of the fish-like body oscillates transversally in the form of traveling wave. The current study is focused on the effects of Reynolds number and the character of midline oscillation on the generation of propulsion force. The investigation indicates that the higher Reynolds number, or higher frequency, or higher amplitude of midline oscillation produces a higher propulsion force. Among the parameters affecting the generation of propulsion force, the amplitude of midline oscillation is the most noticeable factor.

Keywords: Fish swimming; LBM, Immersed boundary; IBVCM

1. Introduction

As a bionics application of fluid dynamics, the investigation of swimming dynamics of undulating fish-like body has provided insight into the details of the fish propulsion. The highly manoeuvrable, power-efficient endurance swimming mechanisms of some fish can potentially provide inspiration for a design of underwater vehicles with similar capabilities. Fish provides useful illustration of propulsor design, swimming modes and body shape. The work of Sfakiotakis et al. (1999) and Colgate and Lynch (2004) gave a good review of these factors.

Many scientists from various backgrounds have attempted to formulate the mathematical and physical models to describe the kinematics of fish (Sfakitakis et al., 1999; Colgate and Lynch, 2004; Alexander, 2003; Koochesfahani, 1989; Lighthill, 1960; Liu, 1996; Liu et al., 1999; Newman, 1973; Schultz and Webb, 2002; Triantafyllou et al., 1993; Videler, 1993; Wassersug and Hoff, 1985). These concepts and data provide significant information about the swimming mechanisms. Among these remarkable works, Wassersug and Hoff (1985) proposed the kinematics for undulatory swimming from observation and experiments, and plotted the specific amplitude along the fish body from the tip to the tail for larvae and cod. Videler (1993) developed a formula for lateral motion of swimming fish by using Fourier terms. Based on their research work and data, some mathematical and computational models were developed (Koochesfahani, 1989; Lighthill, 1960; Liu et al., 1996; Liu and Kaeachi, 1999; Newman, 1973; Videler, 1993).

The fish motion is a moving boundary problem. This brings a great difficulty for numerical simulation. Recently, some new numerical methods were de-

*Corresponding author. Tel.: +65 6516 6476, Fax.: +65 6779 1459
E-mail address: mpeshuc@nus.edu.sg

veloped to simulate fluid flows efficiently. One is the immersed boundary method (IBM) proposed by Peskin (1977). IBM can efficiently simulate flow problems with complex geometry and moving boundaries. Its drawback is that the non-slip condition at the wall cannot be accurately satisfied. As a consequence, some streamlines may pass through the solid body. The other method is the lattice Boltzmann method (LBM) for simulation of incompressible viscous flows. As compared with the Navier-Stokes solvers, the major advantage of LBM is its simplicity and easy implementation. There are no differential equations and resultant algebraic equations involved in LBM. The standard LBM can only be applied on the uniform mesh. To extend it for the application on the non-uniform mesh, Shu et al. (2002) developed the Taylor series expansion- and least square-based LBM (TLLBM).

In this work, we adopt the idea of LBM and IBM to develop the lattice Boltzmann-immersed boundary velocity correction method (LB-IBVCM) for simulation of fish motion. As compared with the conventional IBM, the new approach is easy in implementation and can satisfy the non-slip boundary conditions more accurately. It would be more suitable to simulate problems with moving boundary.

2. Mathmatical modes of undulatory motions

Videler (1993) indicated that swimming by traveling waves of lateral curvature with increasing amplitude is a periodic process and the equations used in physics to describe harmonic motion can be applied to describe steady swimming motion of fish very accurately. He found that the lateral motion can be accurately described by using the first three, odd Fourier terms:

$$y_m(x,t) = \sum_{i=1,3,5} \left[a_i(x)\cos(i2\pi f_i t) + b_i(x)\sin(i2\pi f_i t) \right] \tag{1}$$

where $y_m(x,t)$ is the coordinate of center line in the y-direction, $a_i(x)$ and $b_i(x)$ represent six Fourier coefficients, f_i is the phase speed of the traveling wave, t is time and x is the coordinate in the x-direction. Only the first three odd Fourier terms are used because the movements are laterally symmetric.

Videler (1993) also plotted a series of curves resulted from contributions of various frequencies in Fourier terms. The third and the fifth frequency terms are very small as compared with the first frequency term. Therefore, we omit the higher frequencies and simplify the Eq. (1) as:

$$y_m(x,t) = a_1(x)\cos(2\pi ft) + b_1(x)\sin(2\pi ft) \tag{2}$$

By using the representations:

$$a_1(x) = a_m(x)\cos(2\pi x/\lambda) \quad \text{and}$$
$$b_1(x) = a_m(x)\sin(2\pi x/\lambda) \tag{3}$$

A further formulation can be derived as:

$$y_m(x,t) = a_m(x)\cos(2\pi x/\lambda - 2\pi ft) \tag{4}$$

Here, $a_m(x)$ represents amplitude, λ is wavelength, and f is frequency.

In the kinematics for undulatory swimming proposed by Wassersug and Hoff (1985), the midline of the swimming body oscillates transversally in the form of traveling wave, which in concept is similar to Eq. (4) for lateral motion. The oscillating wave has special amplitude for a specified swimming species. Wassersug and Hoff (1985) plotted the specific amplitude at all points along the body from the tip to the tail for larvae and cod. According to the plots, the amplitude function can be fit out.

3. Lattice boltzmann-immersed boundary velocity correction method

The lattice Boltzmann method (LBM) is a new approach for simulation of incom-pressible viscous flows. Compared to various nu-merical methods for solving the Navier-Stokes equations, the major advantage of LBM is its simplicity and easy implementation. In this work, LBM is applied to give the velocity field on the Cartesian mesh. The lattice Boltzmann equation can be written as:

$$f_\alpha(x + e_\alpha \delta t, t + \delta t) - f_\alpha(x,t) = -\frac{1}{\tau}\left(f_\alpha(x,t) - f_\alpha^{eq}(x,t)\right) \tag{5}$$

where τ is the single relaxation time; f_α is the distribution function; f_α^{eq} is its corresponding equilibrium state; δt is the time step; e_α is the particle velocity. The D2Q9 lattice velocity model is used in the LBM computation, which is defined as:

$$\mathrm{e}_\alpha = \begin{cases} 0 & \alpha = 0 \\ \left(\cos\left[(\alpha-1)\pi/2\right], \sin\left[(\alpha-1)\pi/2\right]\right) & \alpha = 1,2,3,4 \\ \sqrt{2}\left(\cos\left[(\alpha-5)\pi/2+\pi/4\right], \sin\left[(\alpha-5)\pi/2+\pi/4\right]\right) & \alpha = 5,6,7,8 \end{cases} \tag{6}$$

Accordingly, the equilibrium distribution function is given by:

$$f_\alpha^{eq} = w_\alpha \rho \left[1 + 3\mathrm{e}_\alpha \cdot \mathrm{V} + \frac{9(\mathrm{e}_\alpha \cdot \mathrm{V})^2}{2} - \frac{3\mathrm{V}^2}{2} \right] \tag{7}$$

where $w_0 = 4/9$, $w_\alpha = 1/9$ for α =1,2,3,4, w_α = 1/36 for α =5,6,7,8. From conservation laws of mass and momentum, the macroscopic density ρ and fluid velocity V are calculated in terms of the density distribution functions as:

$$\rho = \sum_{\alpha=0}^{8} f_\alpha \quad \mathrm{V} = \frac{1}{\rho}\sum_{\alpha=0}^{8} f_\alpha \mathrm{e}_\alpha \tag{8}$$

In the conventional immersed boundary method (IBM), the surrounding flow near the immersed body is modified through a forcing term to satisfy the non-slip boundary condition. Based on the conventional IBM, we propose a new version, that is, the immersed boundary velocity correction method (IBVCM).

The basic idea of IBVCM is that the body force is not pre-determined. Instead, the velocity at wall interpolated from the surrounding velocity field is forced to satisfy the non-slip boundary condition.

Like the conventional IBM, we limit the effect of the boundary point to a local region in the flow domain. There are two main steps to implement the IBVCM: interpolation and correction. As shown in Fig. 1, with the interpolation equations, the interpolated velocity at the boundary point is:

$$u_{M_x} = u_A + \frac{\Delta_1}{\Delta x}(u_B - u_A) \tag{9}$$

$$v_{M_y} = v_C + \frac{\Delta_2}{\Delta y}(v_B - v_C) \tag{10}$$

Here, $\overline{AM_x} = \Delta_1$, and $\overline{CM_y} = \Delta_2$; Δx and Δy are respectively mesh spacing in the x and y directions.

According to momentum equations, the boundary point M_x only affects the u-velocity correction at two mesh points A and B, and the boundary point M_y only affects the v-velocity correction at two mesh points B and C. Velocity correction between the points A and B is:

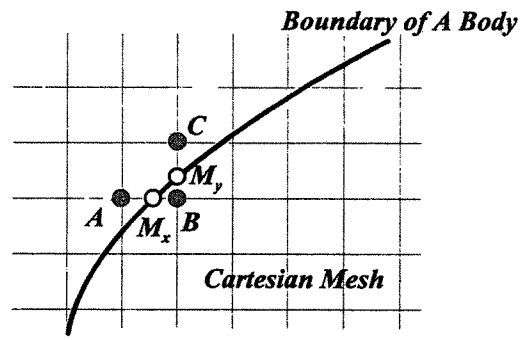

Fig. 1. Cartesian mesh lines, immersed boundary and their intersection points.

$$u' = u_{M_x} - u_A - \frac{\Delta_1}{\Delta x}(u_B - u_A) \tag{11}$$

In a similar manner, the v-velocity correction between the points B and C can be written as:

$$v' = v_{M_y} - v_B - \frac{\Delta_2}{\Delta y}(v_C - v_B) \tag{12}$$

For some cases such that in one mesh spacing, there are more than one intersection points between a mesh line and the boundary, the velocity correction should be applied for all the velocity components.

When IBVCM is combined with LBM, we do not need to modify the Boltzmann equation. The only thing we should do before solving the lattice Boltzmann equation is to set the body force as zero. Then the predicted (intermediate) velocity field on the Cartesian mesh can be obtained by solving the lattice Boltzmann equation. By using the intermediate velocity, the IBVCM can be implemented by velocity interpolation, and velocity correction. After implementing IBVCM, the equilibrium distribution function is re-calculated, and one iteration step is finished.

4. Results and discussions

In the present analyses, we use NACA0012 airfoil as the contour of the fish body. The mesh for NACA-0012 airfoil is shown in Fig. 2. Here the circular symbols are the crossing points of x-direction mesh lines with the boundary, and the triangles are the crossing points of y-direction mesh lines with the boundary.

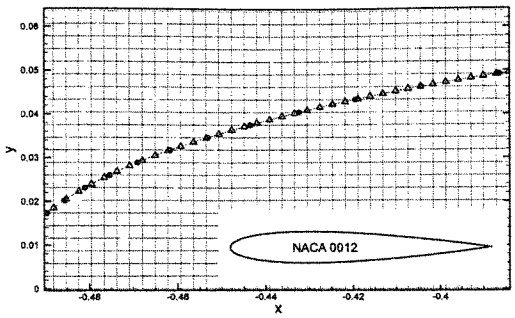

Fig. 2. The mesh line-boundary crossing points with zero angle of attack for NACA0012 airfoil.

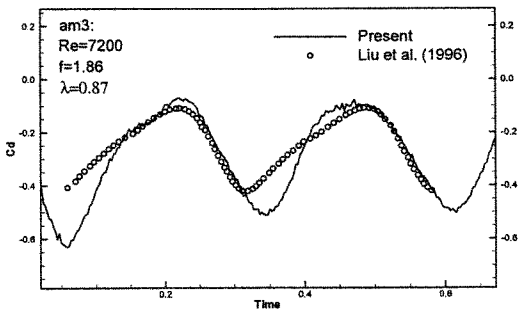

Fig. 3. Comparison: drag coefficient of fish swimming at *Re=7200* and *f=1.86*.

In the present simulation, very fine mesh is used in the region near the fish body, $-0.52 \le x \le 0.52$, and $-0.52 \le y \le 0.52$. It was found that the mesh size of 350×350 used in the body region can provide accurate numerical results.

4.1 Validation of numerical results

At first, we choose a case which has the similar body shape, Reynolds number, frequency and wavelength as used by Liu et al. (1996; 1999) and perform numerical computation to validate the present method. Note that the body shape we adopted for the purpose of validation is a Rana esculenta larva, which is from the book of McDiarmid and Altig (1999). Its maximum thickness is 0.2056L, similar to that of Liu et al. (1996; 1999), where Rana catesbeiana larva has a maximum thickness of 0.2L. Since the present fish shape is not exactly the same as that of Liu et al. (1996; 1999), we can only make a qualitative comparison between two results. The present results and those of Liu et al. (1996; 1999) are shown in Fig. 3. Basically, both results agree well. The difference mainly lies in the early stage. Obviously, after a short time, the propulsion force reveals the periodic feature.

4.2 Effect of amplitude

In our simulation, the amplitude of $a_m(x)$ is denoted by "am3". The amplitude "am3" and "cod" plotted in Fig. 4 were presented by Wassersug and Hoff (1985). The amplitude of "cod" is similar to the description of amplitude given by Videler (1993). The amplitude of $a_m(x)$ can be approximated by a polynomial function:

$$a_m(x) = C_0 + C_1 x + C_2 x^2 + C_3 x^3 + C_4 x^4 \qquad (13)$$

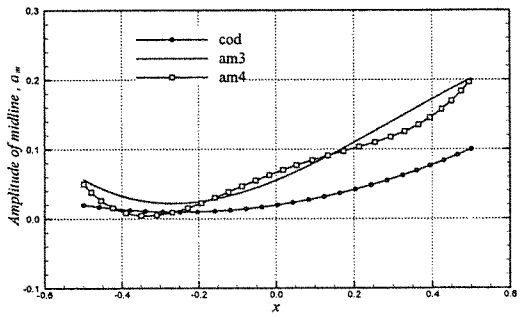

Fig. 4. The amplitude of midline oscillation for Cod and Tadpole.

For "cod" and "am3", we use a cubic polynomial function ($C_4 = 0$). The coefficients in Eq. (13) are calculated from the curve of "am3" and "cod" in Fig. 4 by using a Chebyshev Curve Fitting method. They are summarized in Table 1.

In the work of Liu et al. (1996), and Liu and Kawachi (1999), the amplitude of $a_m(x)$ for tadpole was given by using the spline interpolation from five original maximum amplitudes along the length (L) of the body, which are written as:

$$a_m(-0.5) = 0.05,\ a_m(-0.31) = 0.005,$$
$$a_m(0.116) = 0.04,\ a_m(0.192) = 0.1,\ a_m(0.5) = 0.2 \qquad (14)$$

By using these values in Eq. (14), we can obtain the five coefficients in Eq. (13), which are also included in Table 1. Since the fourth order polynomial is used, we name this amplitude as "am4" to distinguish it from the cubic polynomial amplitude "am3".

Both the curves am3 and am4 in Fig. 4 are amplitudes of tadpoles. The shape of amplitudes for cod (or saithe) is much tenderer and flatter as compared to that of tadpole.

Table 1. The coefficients of polynomial function in Eq. (13) for different amplitudes.

am(x)	C_0	C_1	C_2	C_3	C_4
cod	0.016828	-0.068348	0.223052	-0.088458	0
am3	0.055306	0.22649	0.29446	-0.32656	0
am4	0.05	-0.643378	2.78866	-3.74896	1.75368

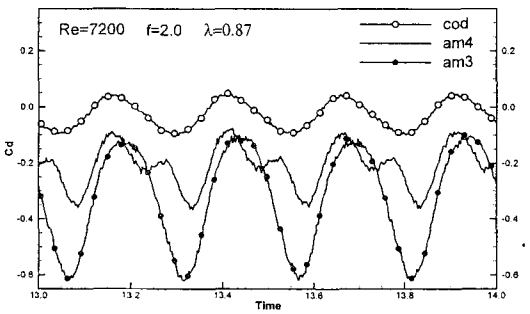

Fig. 5. The drag coefficient for three different amplitudes at *Re=7200*.

The simulation results as shown in Fig. 5 indicate that the amplitudes have a notable effect on the propulsion force (minus drag coefficient). The cod can produce less propelling force without the help of fins and tail blade. For a fish-like body without fins, apparently, the tadpole's swimming mode is a better choice.

By observing the drag coefficients for am3 and am4, the am3 results in bigger propulsion although both am3 and am4 have the same snout amplitude and same tail tip amplitude. The smooth amplitude line of am3 probably brings fish body a balanced and equilibrious vortex generation and shedding. Therefore, we apply the amplitude of am3 in the following study.

4.3 Effect of frequency and wavelength

Experientially, higher frequency results in a bigger propelling force, as long as it is not beyond the physical limit. For the fish swimming, the propulsion force means the negative drag coefficient. At *Re=7200*, when frequency *f=1.3*, the drag coefficient is around zero. The fish swims at a uniform speed (Fig. 6). When frequency increases to *f=1.7*, the fish would speed up because the propelling force (minus drag coefficient) occurs and an accelerating swimming starts. When frequency increases further to *f=2.0*, the propelling force raises greatly. The higher

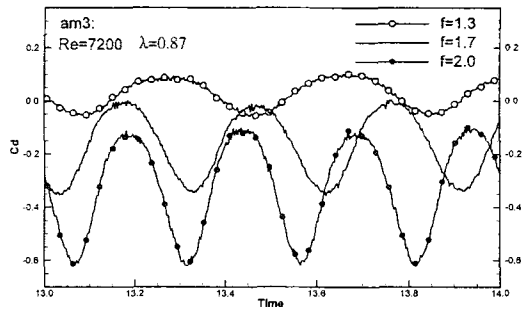

Fig. 6. The drag coefficient of fish swimming with am4 for different frequency at *Re=7200*.

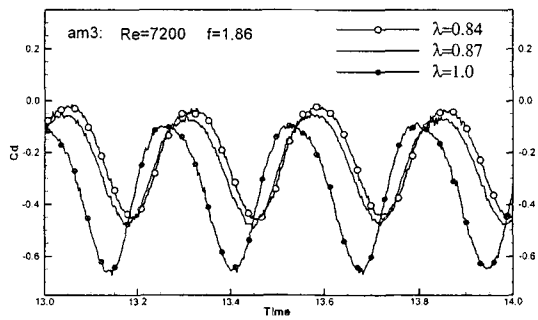

Fig. 7. The drag coefficient of fish swimming with am3 for different wavelength at *Re=7200*.

frequency leads to bigger propelling force, which can be identified easily from Fig. 6.

From the observation and study in previous literatures (Sfakiotakis et al., 1999; Colgate and Lynch, 2004; Liu et al., 1996; Liu and Kawachi, 1973; Newman, 1973) the wavelength λ should be in a range from *0.84* to *0.87*. In this wavelength range, the bigger wavelength produces a little higher peak value of drag coefficient. However, no major difference was found as shown in Fig. 7. The effect cannot be neglected only if the wavelength is close to unity. Thus, in present investigation, a fixed wavelength of *λ=0.87* is adopted.

4.4 Effect of Reynolds number and frequency

To study the combining effects of both Reynolds number and frequency, we performed a series of studies with Reynolds numbers of *Re=3000* and *Re=7200* and different frequencies. Figure 8 shows two curves of *Cd* versus *f* at *Re=3000* and *Re=7200*. Here, *Cd* is an average value in two cycles. The minus *Cd* indicates the gain of propellant force.

At lower Reynolds number, *Re=3000*, the swim-

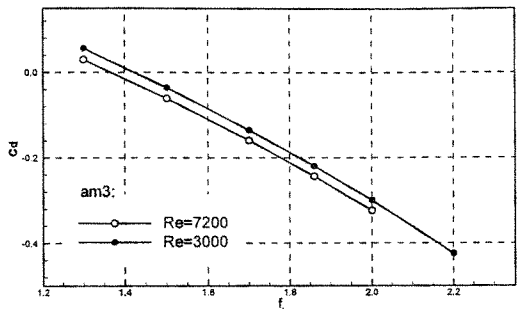

Fig. 8. The average drag coefficients for different frequency and Reynolds number.

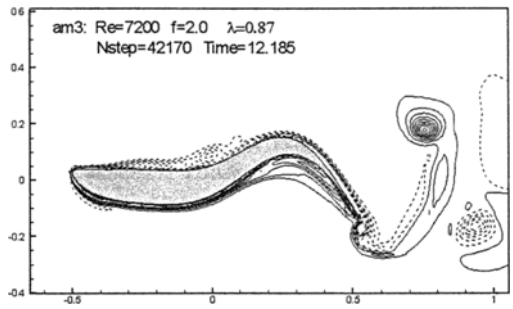

Fig. 10. The vortex contour at location B, for frequency $f=2.0$, $Re=7200$ and $\lambda=0.87$.

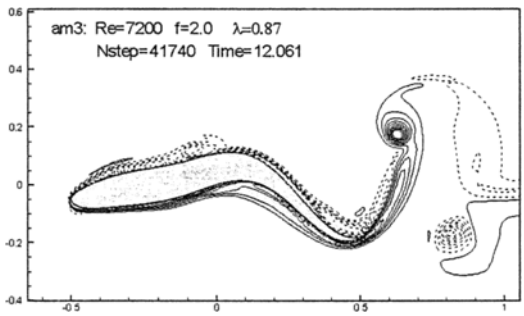

Fig. 9. The vortex contour at location A for frequency $f=2.0$, $Re=7200$ and $\lambda=0.87$.

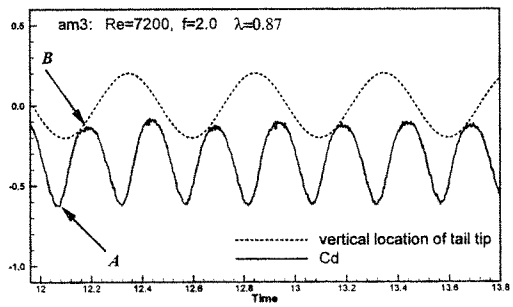

Fig. 11. The drag coefficient and corresponding vertical location of tail tip of fish swimming.

ming fish gains a propelling force only when the frequency arrives or greater than $f=1.43$, while for bigger Reynolds number, $Re=7200$, the propellant force can be gained at a smaller frequency, $f=1.35$. Figure 8 also displays a high effective propulsion situation that the swimming fish could produce an average non-dimensional thrust up to 0.3 or more.

In this higher effective propulsion situation, say, $Re=7200$ *and* $f=2.0$, the vortex contours around the swimming fish in Figs. 9 and 10 show the alternately positive–negative vortex shedding.

The drag coefficient in Fig. 11 shows that the propelling force is gained and reaches peak values twice during each cycle for this case. The vortex contours in Figs. 9 and 10 are extreme examples because they correspond to the bottom peak point A and the top peak point B in Fig. 11, respectively.
Roughly to our sight, both contours are the same in feature. In fact, the vortices attached on the body are opposed in two figures. Two reasons lead to the low propulsion at point A and high propulsion at point B. One is the movement of the body, and another is the vortex.

At point A, the tail-tip of the fish moves down and approaches its peak of amplitude. The movement of tail-tip is slowing down, and tends to stop before changing the direction. At this moment, the vortex shedding from upper and lower surfaces with similar strength and opposite spin directions combines together, and the propulsion is thus decreased.

Similarly, at point B, the tail-tip of the fish moves up from the lowest location and starts to speed-up. The movement of tail-tip is accelerating. At this moment, the attached vortex on the upper surface is pulled and weaker, thus the vortex drag is decreased, and propulsion is increased.

In one movement cycle of the fish tail tip, the peak propulsion occurs twice. One occurs after the tail tip arrives at the lowest location and another one occurs after the tail tip arrives at the highest location.

5. Conclusions

The present numerical simulation confirms that IBVCM method is an effective approach in capturing the flow feature and wake structure, even for the problem with moving boundary.

The current study indicates that fish can gain its

propulsion easier at a higher Reynolds number. A critical frequency (smallest frequency) can be obtained to gain a non-zero propelling force for a given Reynolds number. Generally, the higher the frequency, the bigger the propelling force. However, the frequency has a biological limit, which is usually smaller than the convergent limit of computational simulation or experimental simulation.

The oscillating midline of the swimming body is modeled by a traveling wave. The oscillating wave is described by a cosine function mathematically in present investigation. The study indicates that the amplitude of midline oscillation has the most noticeable effect on the propulsion force. Apparently, higher amplitude, especially, higher tail tip amplitude leads to greater propulsion. Of course, there is a biological limit to the amplitude. On the other hand, the arrangement of the amplitude along the midline of fish body is also very important. At the same tail tip amplitude, a smooth amplitude curve along the midline of fish body means a balanced, equilibrious and harmonistic swimming manner and will produce higher propulsion.

References

Alexander, R. McN., 2003, "Principles of Ani-mal Locomotion," *Princeton: Princeton University Press.*

Colgate, J. E. and Lynch, K. M., 2004, "Me-chanics and Control of Swimming: a Review," *IEEE J. of Oceanic Engineering,* Vol. 29(3), p. 660.

Koochesfahani, M. M., 1989, "Vortical Patterns in the wake of an Oscillating Airfoil," *AIAA J.*, Vol. 27(9), p. 1200.

Lighthill, M. J., 1960, "Note on the Swimming of Slender Fish," *J. Fluid. Mech.*, Vol. 9, p. 305.

Liu, H. and Kawachi, K., 1999, "A numerical Study of Undulatory Swimming," *J. Comput. Phys.*, Vol. 155, p. 223.

Liu, H., Wassersug, R. and Kawachi, K., 1996, "A Computational Fluid Dynamic Study of Tad-pole Swimming," *J. Exp. Biol.*, Vol. 199(6), p. 1024.

McDiarmid, R. W. and Altig, R., 1999, *Tadpoles: the biology of anuran larvae.* Chicago and London: University of Chicago Press.

Newman, J. N., 1973, "The Force on a Slender Fish-like Body," *J. Fluid Mech.*, Vol. 58(4), p. 689.

Peskin, C. S., 1977, "Numerical Analysis of Blood Flow in the Heart," *J. Comp. Phys.*, Vol. 25, p. 220.

Schultz, W. W. and Webb, P. W., 2002, "Power Requirements of Swimming: do new Methods Resolve Old Questions?" *Integr. Comp. Biol.*, Vol. 42, p. 1018.

Sfakiotakis, M., Lane, D. M. and Davies, J. B. C., 1999, "Review of fish swimming Modes for Aquatic Locomotion," *IEEE J. Oceanic Eng.*, Vol. 24, p. 237.

Shu, C., Niu, X. D. and Chew, Y. T., 2002, "Taylor Series Expansion- and least Square-based Lattice Boltzmann Method: Two-Dimensional For-mulation and its Applications," *Phys. Rev.* E 65, 036708.

Triantafyllou, G. S., Triantafyllou, M. S. and Grosenbaugh, M. A., 1993, "Optimal Thrust Development in Oscillating foils with Application to Fish Propulsion," *J. Fluid Struct.*, Vol. 7, p. 205.

Videler, J. J., *Fish Swimming*, Chapman & Hall, London.

Wassersug, R. and Hoff, K., 1985, "The Ki-nematics of Swimming in Anuran Larvae," *J. Exp. Biol.*, Vol. 119, p. 1.